J. Fluid Mech. (2004), *vol.* 510, *pp.* 131–144.
DOI: 10.1017/S0022112004009243 Printed in the United Kingdom

Active management of naturally separated flow over a solid surface. Part 2. The separation process

By A. DARABI AND I. WYGNANSKI

Department of Aerospace Engineering, University of Arizona, Tucson, AZ 85 721, USA

(Received 20 April 2003 and in revised form 24 February 2004)

The controlled separation of flow from an inclined straight flap at high inclination angles was investigated experimentally. The separation process was initiated by an abrupt change in the excitation emanating from a slot at the flap shoulder. A complete cessation of the actuation resulted in formation of a large vortex above the flap akin to the familiar 'dynamic stall vortex' (DSV) seen over oscillating airfoils in pitch. The DSV temporarily increased the aerodynamic load over the flap before it dropped to its low separated value. The duration of this overload decreased as the flap inclination increased. The use of periodic excitation during separation slowed down the rate of separation and changed its character depending on the amplitude and the frequency used. Forcing separation by switching the excitation to a high frequency ($3 < F^+ < 8$) reduced or even eliminated the increase in flap loading that is associated with the DSV. A switch to low frequencies ($F^+ < 1$) extended the duration of separation and increased the transient overload during the initial stage of the process.

1. Introduction

Flow separation from a solid surface in steady two-dimensional flow occurs where the skin friction vanishes. In an unsteady flow, however, the location of separation may be more vague, since in this case vanishing skin friction and vanishing velocity do not necessarily coincide (Sears 1956). The flow over thin airfoils may enclose a long leading-edge bubble that increases rapidly in length when the incidence angle is increased, bringing about sudden detachment of the flow as it bursts. This is accompanied by a large loss of lift and a sharp increase in form drag. Therefore, abrupt stall normally starts near the leading edge of the airfoil. On thick airfoils, the flow separates first near the trailing edge where the boundary layer is most depleted of its momentum in the direction of streaming. If the increase of incidence is slow, the separation location follows suit by propagating slowly upstream, resulting in a gentle stall.

When an airfoil oscillates in pitch at a high rate to an excessive incidence angle, a dynamic stall vortex is generated either toward the end of the upstroke part of the cycle (if the static stall angle is exceeded) or at the beginning of the downstroke (if the rate of pitch is also excessive). The generation of the dynamic stall vortex on a pitching airfoil and the means to prevent it (Greenblatt *et al.* 2001) has received considerable attention in view of its significance to rotor aerodynamics and the limitation that it imposes on the forward speed of helicopters. The same phenomenon can be beneficial when used to increase the manoeuvrability of aircraft, particularly unmanned ones.

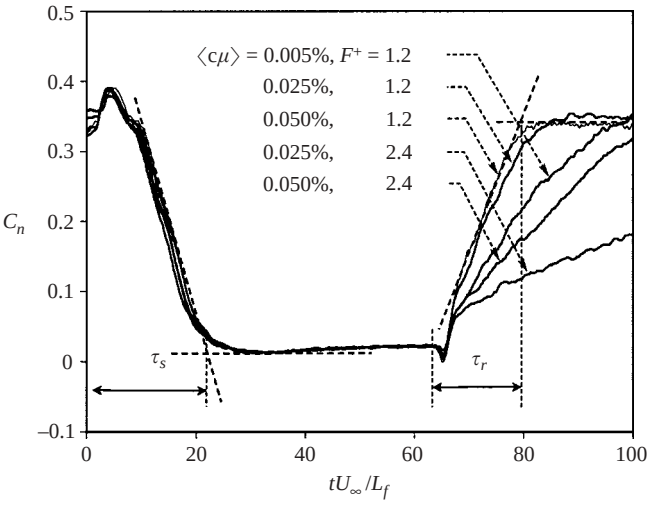

FIGURE 1. The evolution of C_n during a sequence of uncontrolled separation followed by forced reattachment; $Re_L = 1.65 \times 10^5$, $\Delta\alpha_s = 5^\circ$.

Thus, understanding and controlling the dynamic processes associated with separation are important.

The present investigation attempts to elucidate some of the factors affecting flow separation caused by pure oscillatory control with no concomitant change in the inclination angle of the aerodynamic surface. The experiment started with turbulent flow that was forcefully attached to a straight flap deflected at angles exceeding the natural separation angle $\alpha_{s0}(\alpha_{s0} \approx 18^\circ$ for the flap length used; see Part 1, Darabi & Wygnanski 2004). At a constant excessive flap deflection angle $\Delta\alpha_s(=\alpha - \alpha_{s0})$, the excitation parameters $\{F^+, \langle c\mu \rangle\}$ were abruptly changed from a level that maintained the flow attached to a level that could do so no longer, resulting in a controlled process of separation. It is demonstrated that the separation process can be initiated and reversed without moving the control surface, thereby generating arbitrary forces and hinge moments of any prescribed duration.

The detailed description of the experimental set-up is given in Part 1.

2. The process of flow separation

2.1. *Uncontrolled separation*

A sudden termination of excitation is the simplest way to initiate separation of forcefully attached flow, providing the fundamental response of the system to a step-change in forcing. We shall refer to this case as an *uncontrolled* separation process. The changes in the normal force coefficient, C_n, resulting from a cessation of the excitation at $\tau \equiv tU_\infty/L_f = 0$ that is followed by forced reattachment initiated at $\tau = 64$ are illustrated in figure 1. Five forcing conditions are considered which provide different flap loads during the steady state preceding the separation, as well as different authority over the reattachment process. The Reynolds number and the deflection in excess of the natural separation angle are $Re_L = 165\,000$ and $\Delta\alpha_s = 5^\circ$, respectively.

The progression of separation after the cessation of excitation comprises two stages. First, the flap load increases, reaching a peak value at $\tau \approx 5$. This increase in load is analogous to the lift augmentation during the formation of the dynamic stall vortex

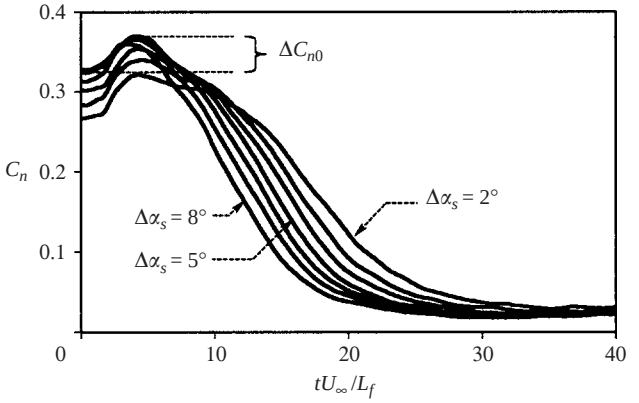

FIGURE 2. The effect of $\Delta\alpha_s$ on the evolution of C_n during uncontrolled separation; $Re_L = 1.65 \times 10^5$, $F_r^+ = 1.2$ and $\langle c\mu \rangle_r = 0.05\%$.

(DSV) over an airfoil oscillating in pitch (McAlister *et al.* 1982; Greenblatt *et al.* 2001). In a second stage, the flap load drops almost linearly to its low separated state value. For all five cases considered in figure 1, the maximum C_n attained and the time required to attain it are independent of the initial conditions of excitation and the C_n values prevailing prior to the termination of the excitation. The total dimensionless time required to complete the uncontrolled separation process at $\Delta\alpha_s = 5°$ is $\tau_{s0} \approx 21$, and it is slightly longer than the time τ_r required to force the flow to reattach at optimal conditions (the difference between the two times increases when $\Delta\alpha_s$ decreases). As illustrated in figure 1, the general separation time τ_s was defined in a similar manner to τ_r by letting the maximum (absolute) slope $(\mathrm{d}C_n/\mathrm{d}\tau)_{max}$ intersect the extension of the final steady state value of C_n.

The effect of flap inclination on the evolution of the normal force, C_n, during uncontrolled separation is demonstrated in figure 2. All other control parameters prior to the cessation of excitation were kept constant in these tests. Specifically, $F_r^+ = 1.2$, $\langle c\mu \rangle_r = 0.05\%$ and $Re = 165\,000$ (the subscript r is used to denote the initial reattached conditions at $\tau < 0$). The primary effect of the increase in $\Delta\alpha_s$ is the acceleration of the separation process, caused mostly by a decrease in the duration of the DSV. During the second stage of separation, C_n decays with time at a rate that is almost independent of $\Delta\alpha_s$. There are hardly any variations in the maximum increase in C_n above the initial steady-state values owing to changes in flap inclination ($\Delta C_{n0} \approx 20\%$). The overall decrease in the uncontrolled separation time with $\Delta\alpha_s$ is totally independent of the initial flow conditions (figure 3) and of Reynolds number in the range of values tested (8.2×10^5 to 20.7×10^5).

The initial excess load on the flap is examined by tracking the changes in the spatial distribution of the pressure coefficient, C_p, at several time steps after the cessation of excitation (figure 4). When the pressure distribution at $\tau = 0$, corresponding to the initial forcefully attached flow, is compared to that measured at $\tau = 5$, we observe that the area under the curve at $\tau = 5$ had increased in spite of the reduction in suction near the leading edge of the flap. This causes an increase in flap load and in the hinge moment while shifting the centre of pressure closer to the trailing edge. The independence of the uncontrolled separation process from the initial conditions is emphasized in figure 5 by comparing three vastly different initial C_p distributions at two discrete stages of the separation process. Solid lines represent distributions at the

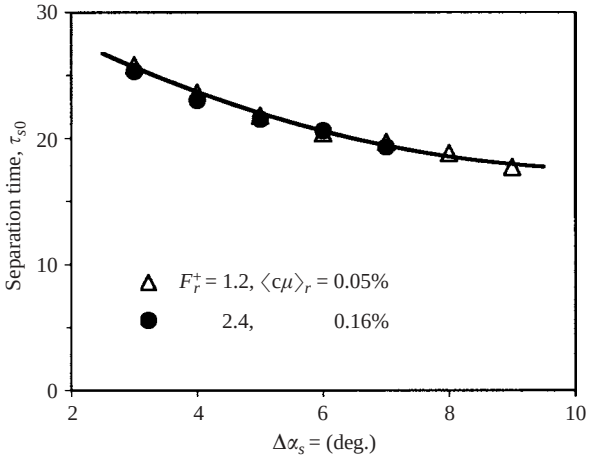

FIGURE 3. The uncontrolled separation time as a function of the flap deflection angle for two different initial conditions.

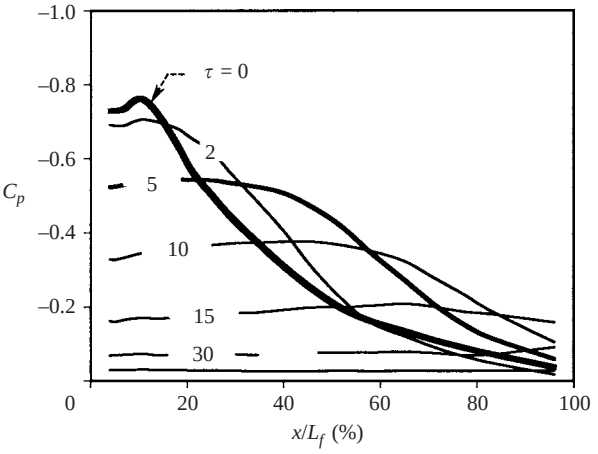

FIGURE 4. Spatial distribution of C_p at different time steps during unforced separation; $Re_L = 1.24 \times 10^5$, $\Delta\alpha_s = 5°$, $F_r^+ = 2.4$, $\langle c\mu\rangle_r = 0.05\%$.

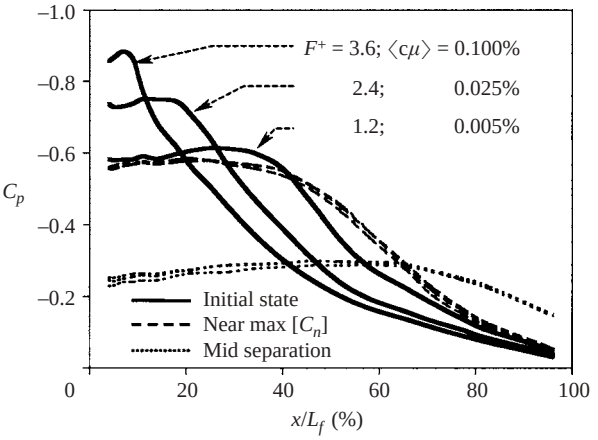

FIGURE 5. Distributions of the wall pressure coefficient at three stages during unforced separation, for different initial conditions.

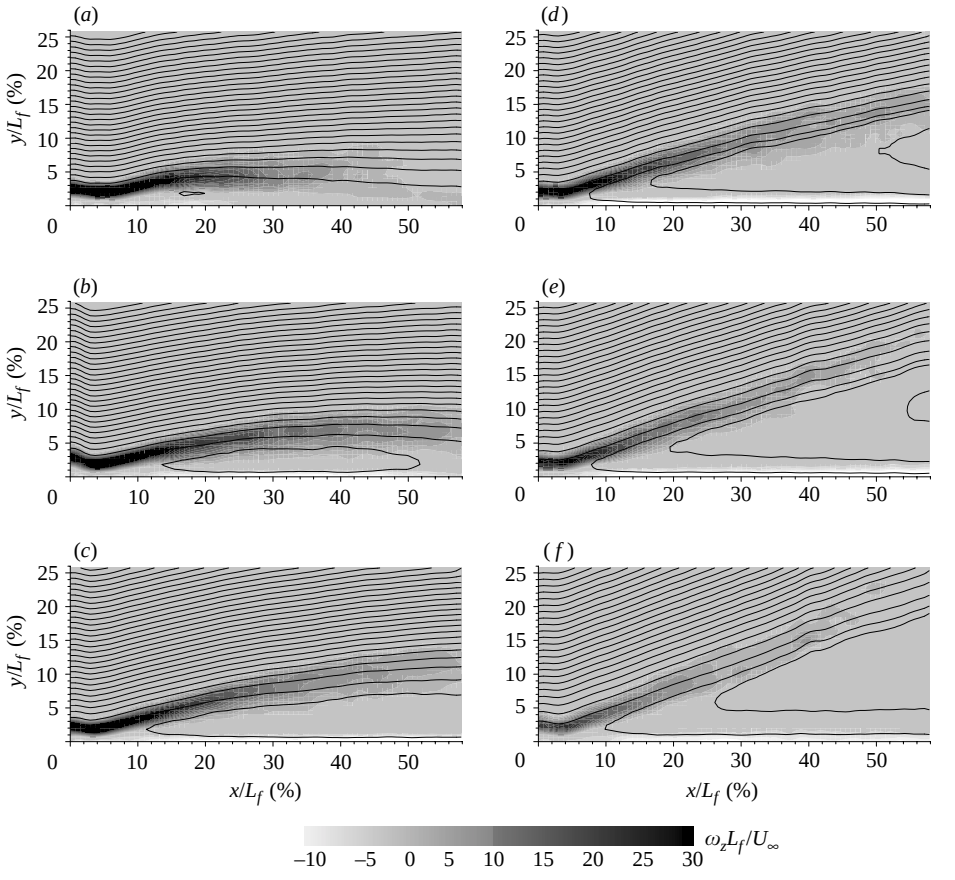

FIGURE 6. Mean vorticity and streamlines at different stages during uncontrolled separation; $Re_L = 1.24 \times 10^5$, $\Delta\alpha_s = 5^\circ$, $F_r^+ = 1.2$, $\langle c\mu \rangle_r = 0.02\%$. (*a*) $\tau = 0$, $t = 0$ ms. (*b*) $\tau = 2.5$, $t = 80$ ms. (*c*) $\tau = 5$, $t = 160$ ms. (*d*) $\tau = 7.5$, $t = 240$ ms. (*e*) $\tau = 12.5$, $t = 400$ ms. (*f*) $\tau = 25$, $t = 800$ ms.

initial steady attached conditions, hatched lines correspond to the stage at which C_n attains its maximum level ($\tau \approx 5$) and dotted lines represent the C_p distributions prior to the completion of separation ($\tau \approx 13$). It is clear that the uncontrolled separating flow always evolves in the same manner regardless of its initial pressure distribution, provided that $\tau > 5$. At this stage, all the C_p distributions coalesce onto a single curve, which closely resembles the steady-state conditions that maintained the flow on the verge of separation with a leading-edge bubble extending over 60% of the flap chord.

Figure 6 compares the average evolution of the flow measured by a PIV during uncontrolled separation. The various shades of grey represent contours of constant spanwise vorticity. They are overlaid by equally spaced streamlines. The separation process starts with the growth of the small recirculation region that was initially centred at $x/L_f \approx 18\%$ (figure 6*a*) during the forcefully attached flow. As the bubble grows, the point of maximum streamline curvature moves downstream until at approximately $\tau = 5$ it is located around the mid-chord of the flap. At later times, the bubble opens up at the trailing-edge region of the flap, allowing the shear layer to detach almost uniformly away from the surface. Therefore, the unforced separation begins at the flap leading edge and progresses through the growth of the recirculation zone.

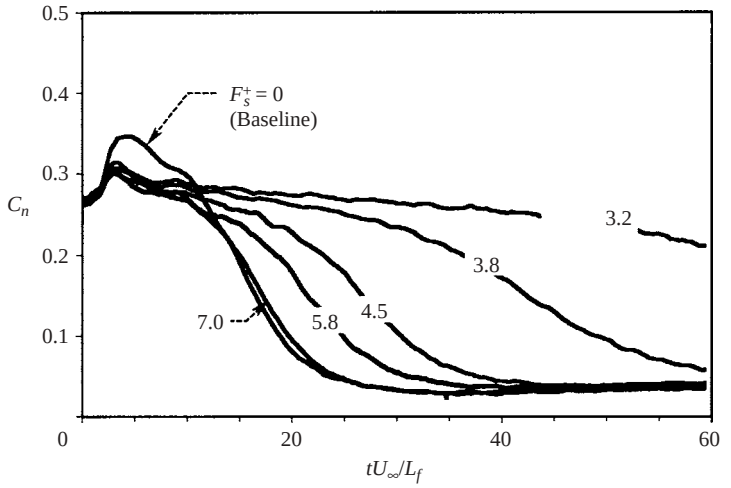

FIGURE 7. C_n during separation at high frequency – frequency effect (small initial bubble); $Re_L = 1.24 \times 10^5$, $\Delta\alpha_s = 5^\circ$, $F_r^+ = 2.4$, $\langle c\mu \rangle_r = 0.1\%$, $\langle c\mu \rangle_s = 0.01\%$.

2.2. *Controlled separation – general response*

When the control parameters used to keep the flow attached are abruptly changed at $\tau = 0$ to values of F_s^+ and $\langle c\mu \rangle_s$ that can no longer sustain attached flow, *controlled* separation commences. There are significant differences between the flow that separates at high or at low F_s^+ (see Nishri 1995); therefore, we consider the two processes separately.

The changes in C_n during separation resulting from a shift in excitation to higher and higher frequencies are shown in figure 7. The measurements were conducted at a constant deflection angle ($\Delta\alpha_s = 5^\circ$) and Reynolds number ($Re_L = 1.24 \times 10^5$), with initial excitation at $F_r^+ = 2.4$ and $\langle c\mu \rangle_r = 0.1\%$ that featured a relatively small leading-edge bubble. The frequencies used to force separation ranged from $F_s^+ = 3.2$ to $F_s^+ = 7$, while the amplitude remained constant at $\langle c\mu \rangle_s = 0.01\%$. The use of high-excitation frequencies clearly slows down the separation process, underlining the fact that cessation of actuation is the fastest possible way to bring about flow separation. Switching to frequencies that are slightly higher than a threshold value of $F_s^+ \approx 3$, results in exceedingly slow separation (see result for $F_s^+ = 3.2$). Increasing F_s^+ speeds up the process, so that, for $F_s^+ = 7$, the separation time of the controlled flow is almost identical to that achieved by the cessation of forcing. Another important aspect of separation at higher frequency is the reduction of the transitory increase in C_n. For all cases considered in figure 7, the C_n excursion beyond the attached value is approximately halved (from $\Delta C_n \approx 0.08$ to $\Delta C_n \approx 0.04$) compared to the unforced case. In this respect, the selected frequency of the excitation plays only a minor role.

Figure 8 illustrates the effect of excitation amplitude on the controlled separation. The initial flow was attached at $F_r^+ = 1.2$ and $\langle c\mu \rangle_r = 0.02\%$ and separation was forced by switching to $F_s^+ = 5.1$, with amplitudes ranging from $\langle c\mu \rangle_s = 0.005\%$ to $\langle c\mu \rangle_s = 0.08\%$. The forcing conditions at $\tau < 0$ created a large re-circulation zone above the flap (see figure 5). The increase in amplitude slows down the separation, as does a decrease in the frequency, and it reduces C_n during the early stages of separation. More importantly, the data demonstrate the great sensitivity of the separating flow to the smallest level of excitation. Application of $\langle c\mu \rangle_s = 0.005\%$ suffices, under current conditions, to fully eliminate the transient growth in the C_n.

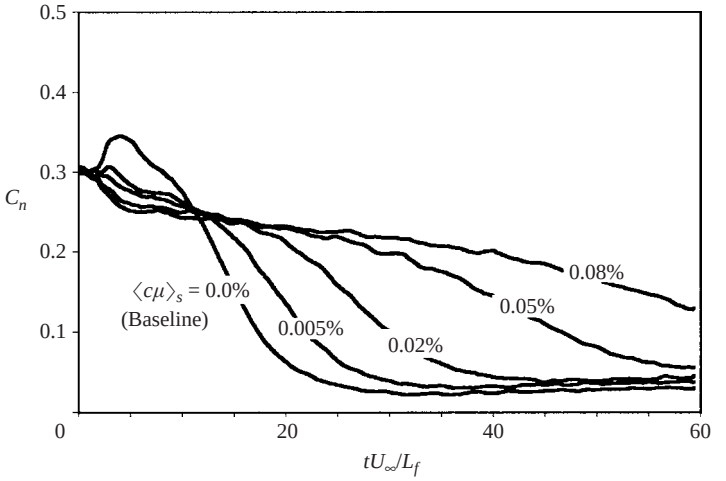

FIGURE 8. C_n during separation at high frequency – Amplitude effect (large initial bubble); $Re_L = 1.24 \times 10^5$, $\Delta\alpha_s = 5°$, $F_r^+ = 1.2$, $\langle c\mu\rangle_r = 0.02\%$, $F_s^+ = 5.1$.

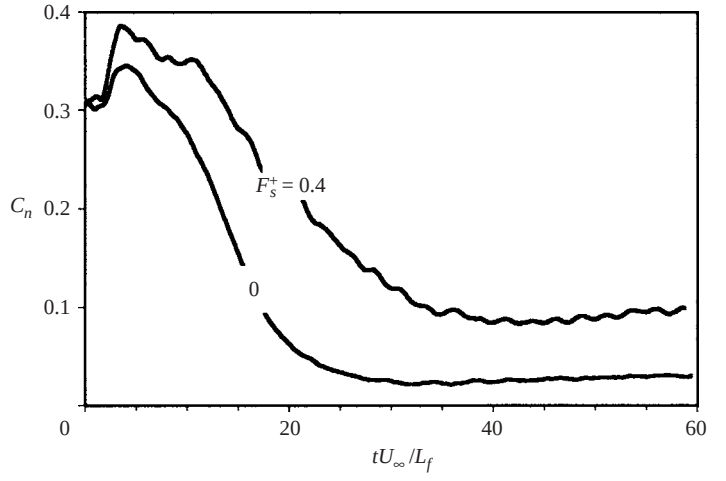

FIGURE 9. C_n during separation forced at low frequency; $Re_L = 1.24 \times 10^5$, $F_r^+ = 1.2$, $\langle c\mu\rangle_r = 0.02\%$, $F_s^+ = 0.4$, $\langle c\mu\rangle_s = 0.02\%$.

Flow separation resulting from a shift to a low-frequency excitation is demonstrated in figure 9. The measurements started with an attached flow that encloses a fairly large bubble, corresponding to $F_r^+ = 1.2$ and $\langle c\mu\rangle_r = 0.02\%$. Separation was caused by switching to $F_s^+ = 0.4$, while maintaining the amplitude at its initial level of $\langle c\mu\rangle_s = 0.02\%$. Although this operation also slows down the separation process, it differs fundamentally from a switch to high frequency in all other aspects. First, using $F_s^+ = 0.4$ doubled the transient C_n excursion, in contrast to its elimination at most high frequencies. Secondly, it increased the time that C_n was elevated (i.e. the time required for C_n to return to its steady-state attached value). In the case presented, the elevated time increased from $\Delta\tau \approx 6$ for the unforced separation to $\Delta\tau \approx 12$ for the forced one. Unlike the separation caused by a switch to a high frequency, here the final separated steady state retains a certain level of load on the flap (figure 9).

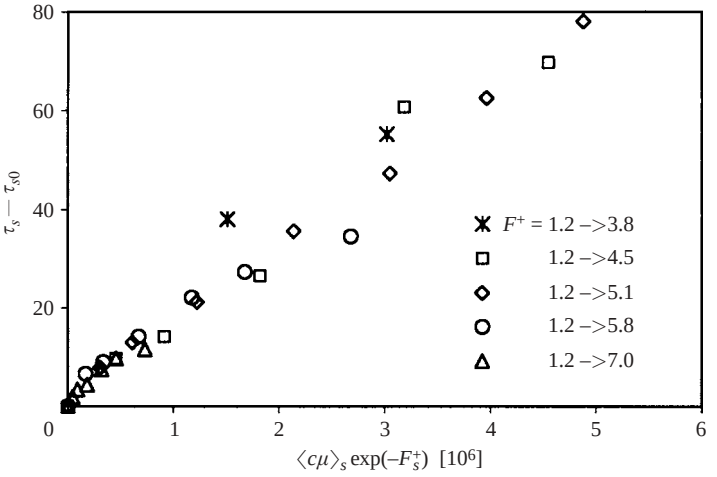

FIGURE 10. Separation time in excess of the uncontrolled process as a function of a combined forcing parameter.

Figure	Process	F_r^+		F_s^+	$\langle c\mu \rangle_r$%		$\langle c\mu \rangle_s$%
11(*a*)	Separation at low frequency	1.2	→	0.4	0.02	→	0.02
11(*b*)	Separation at high frequency	1.2	→	7.0	0.02	→	0.01
11(*c*)	Separation at high frequency	2.4	→	4.5	0.10	→	0.01

TABLE 1. Variation in conditions of excitation.

Thus, the range of excitation frequencies that are useful for controlling the rate of separation without the generation of detrimental hinge moments is roughly $3 < F_s^+ < 8$. Below this range, the flow remains attached, while above it, it separates at the same rate as the undisturbed case. The amplitude of the excitation has a similar effect in controlling the duration of the process. It turned out that within the indicated frequency range, the slowdown in the rate of separation $\tau_s - \tau_{s0}$ (i.e. the time in excess of the uncontrolled process) varies exponentially with F_s^+. By contrast, the dependence of $\tau_s - \tau_{s0}$ on the forcing amplitude at a fixed F_s^+ is approximately linear within the applied range. Incorporating the two observations yields a single dimensionless control variable: $\langle c\mu \rangle_s \exp(-F_s^+)$. Figure 10 illustrates the implementation of this empirical relation to several sets of measurements having common initial conditions ($F_r^+ = 1.2$, $\langle c\mu \rangle_r = 0.02\%$). Despite some scatter that may be attributed to uncertainty in measuring $\langle c\mu \rangle$, the simplification seems to be valid as most of the data fall onto a single curve.

2.3. *Controlled separation – the flow field*

The manner in which the oscillatory control enhances or virtually eliminates the DSV and the ensuing changes in the hinge moments may be readily appreciated by inspecting the spatial surface pressure distributions at prescribed time steps (figue 11). All pressure measurements were carried out at $Re_L = 1.24 \times 10^5$ and a constant deflection angle of $\Delta\alpha_s = 5°$, but they vary in the initial and in the final conditions of excitation, as shown in table 1.

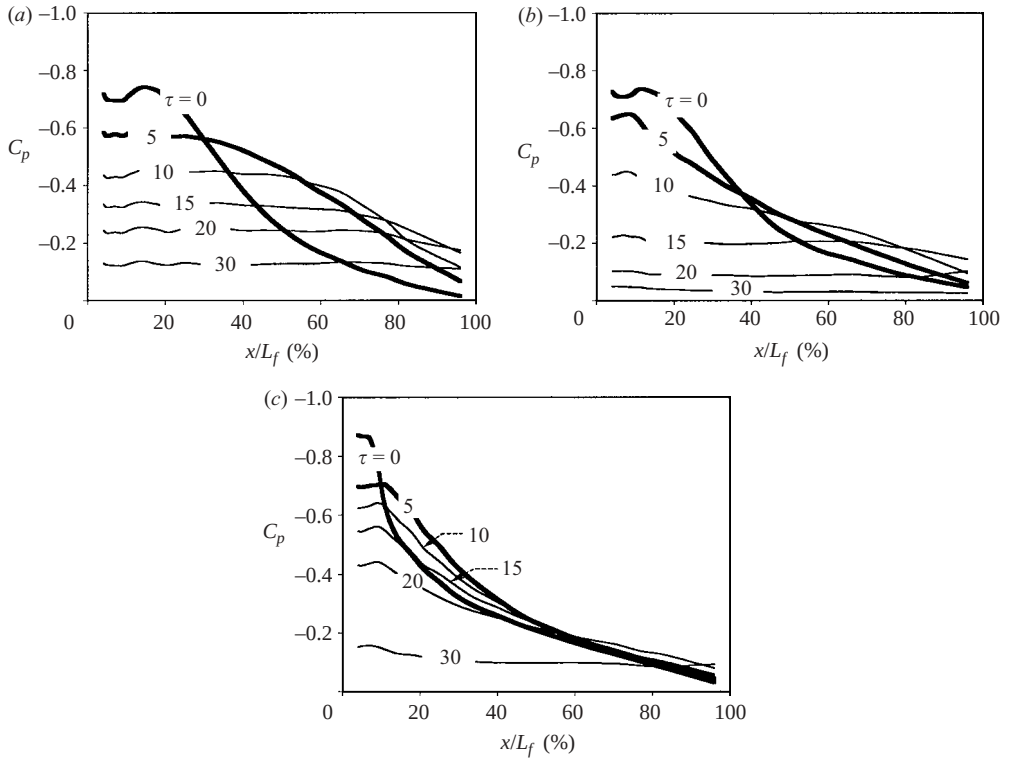

FIGURE 11. Spatial distribution of the pressure coefficient during controlled separation at different frequencies; $Re_L = 1.24 \times 10^5$, $\Delta\alpha_s = 5°$. (*a*) $F_s^+ = 0.4$; (*b*) 7.0; (*c*) 4.5.

During the separation process, caused by a shift to a low frequency (figure 11*a*), a very large recirculating zone is created over the flap that attains a maximum size around $\tau = 5$. The recirculation zone spans at this stage over most of the flap surface, accentuating the phenomenon observed during unforced separation (figure 4). The pressure distributions observed between $\tau = 0$ and $\tau = 5$ during a shift to $F_s^+ = 7$ do not possess a large constant low-pressure region indicative of the presence of a bubble or a DSV (figure 11*b*). The switch to a somewhat lower frequency, $F_s^+ = 4.5$ (figure 11*c*), does not indicate a strong presence of the DSV either, but it preserves better the pressure gradient along the flap throughout the process.

Two sets of phase-locked PIV measurements carried out during the controlled separation process are presented by means of isodynes overlaid by streamlines in figures 12(*a*) and 12(*b*). The initial control parameters, $F_r^+ = 1.2$ and $\langle c\mu \rangle_r = 0.02\%$, are identical to those used for monitoring the separation resulting from the cessation of excitation (figure 6). Figure 12(*a*) represents the changes observed in the flow resulting from a switch in the frequency to $F_s^+ = 7$ (corresponding to pressure data shown in figure 11*b*). The isodynes in the figure are lumpy owing to the phase locking, revealing the smaller scales of the eddies generated by the high-frequency excitation. Inspection of frames (i), (ii) and (iii) suggests that the progression of separation during the period $0 < \tau < 5$ is very slow when compared to the unforced case. The flow responds to the increase in frequency first by a transient decrease in the boundary-layer thickness near the leading edge of the flap (figure 12*a* ii), shrinking the pre-existing re-circulation zone that is initially centred at $x/L_f \approx 18\%$ (figure 6*a*).

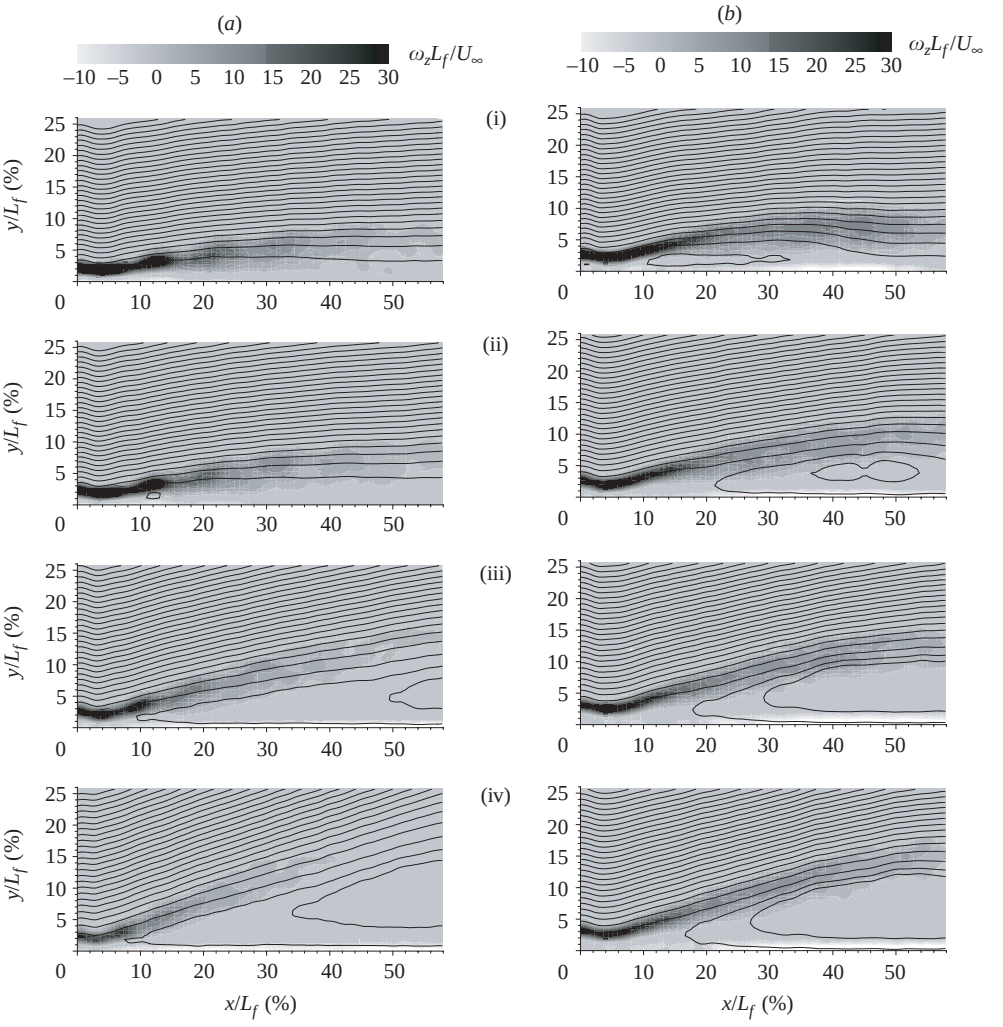

FIGURE 12. Mean vorticity and streamlines during separation at high and low frequency; $\Delta\alpha_s = 5°$, $F_r^+ = 1.2$, $\langle c\mu\rangle_r = \langle c\mu\rangle_s = 0.02\%$: (*a*) $F_s^+ = 7$, (*b*) $F_s^+ = 0.4$, (i) $\tau = 2.5$, $t = 80$ ms. (ii) $\tau = 5$, $t = 160$ ms. (iii) $\tau = 12.5$, $t = 400$ ms. (iv) $\tau = 25.0$, $t = 800$ ms.

This shrinkage is consistent with the redistribution of C_p, taking place near the leading edge of the flap during $0 < \tau < 5$ (figure 11*b*). Further downstream, the streamlines detach uniformly from the flap surface, creating a shallow elongated recirculation region that very quickly spans most of the flap length (figure 12*a* iv). Starting at $\tau \approx 5$, the general orientation of the streamlines changes gradually until it coincides with the direction of the upstream flow upon the completion of separation. These observations demonstrate that high-frequency excitation suppresses the growth of the recirculation zone, thereby, preventing leading-edge separation of the flow. The relatively small energetic eddies that keep the flow attached nevertheless weaken rapidly in the direction of streaming, resulting in insufficient amplitudes near the trailing edge of the flap. This reinforces the notion that separation due to excitation at high frequency begins at the trailing edge of the flap and gradually propagates upstream (Nishri & Wygnanski 1998).

The phase-locked PIV measurements made during separation resulting from a switch to $F_e^+ = 0.4$ (figure 12(*b*)) reveal the general similarity existing between this process and that resulting from the cessation of excitation. Both processes clearly involve a progressively growing recirculation zone that originates near the flap hinge. They differ, however, in the spatial extent and the relative thickness of this zone. At comparable times, separation at low-frequency excitation encloses a bubble that is much larger than the one during the unforced separation. The differences become even more prominent at later stages of the process, when the controlled curvature of the streamlines, accounting for the residual steady loading over the flap, remains unchanged. We may conclude that a switch to a low-frequency excitation causes the flow to commence separation near the leading edge of the flap. It allows extensive growth of the recirculation zone because such excitation is completely inefficient near the flap shoulder. Unlike in the uncontrolled case, low-frequency excitation generates large-amplitude perturbations near the trailing edge of the flap that concomitantly restrain flow separation in this area.

The amplitude of the phase-locked and ensemble-averaged surface pressure fluctuations measured during two different separation processes are shown in figure 13. Temporal changes in the local amplitudes were obtained by Fourier decomposition of short segments in the time records of $\langle C_p \rangle$ (see § 3.3 in Part 1). In the first case, the amplitude was lowered to a level that could not sustain attached flow while keeping the frequency constant at $F^+ = 1.2$ (figure 13*a*). This simulated the process of uncontrolled separation. The small perturbations at this frequency undergo spatial amplification near the flap hinge at all times shown; however, the region at which the fluctuation became amplified shrank with increasing time (from $x/L_f \approx 0.5$ to $x/L_f \approx 0.25$) and the maximum amplitude attained became lower. Stability considerations at the appropriate frequency and phase velocity yield similar results. The decay of the maximum amplitude of the pressure fluctuations with increasing time is attributed in part to the increasing distance between the shear layer and the solid surface during the separation process. The separation resulting from a switch to $F^+ = 0.4$ (figure 13*b*) shows no signs of temporal decay of the pressure fluctuations. In this case, the maximum amplitude observed near the trailing edge of the flap increases initially ($\tau < 9.4$) before settling down to a level that seems to be independent of time. The initial increase in amplitude may stem from the transient growth of the average bubble (or DSV). Here, the size of the passing eddies is commensurate with the distance between the shear layer and the solid surface near the trailing edge of the flap, which is likely to contribute to the residual load on the flap (figure 9).

2.4. *Incomplete separation followed by forced reattachment*

So far, we have described events leading to complete state transitions. We may control the instantaneous forces and moments exerted by a flap (or other aerodynamic surface) by continuously changing the imposed periodic excitation. An effective control scheme is likely to involve frequent switching between the processes before they actually reach their end states. If the flow over an inclined surface near a tip of a wing were controlled, it would provide an adjustable rolling moment to an aeroplane, similar to a conventional aileron. It will do so without moving the surface at maximum rates that are commensurate with the controlled durations of the separation and the reattachment processes.

A few tests were made to investigate how a flow, undergoing controlled separation from $F_r^+ = 1.2$ to $F_s^+ = 7$, recovers when the oscillatory excitation is restored to

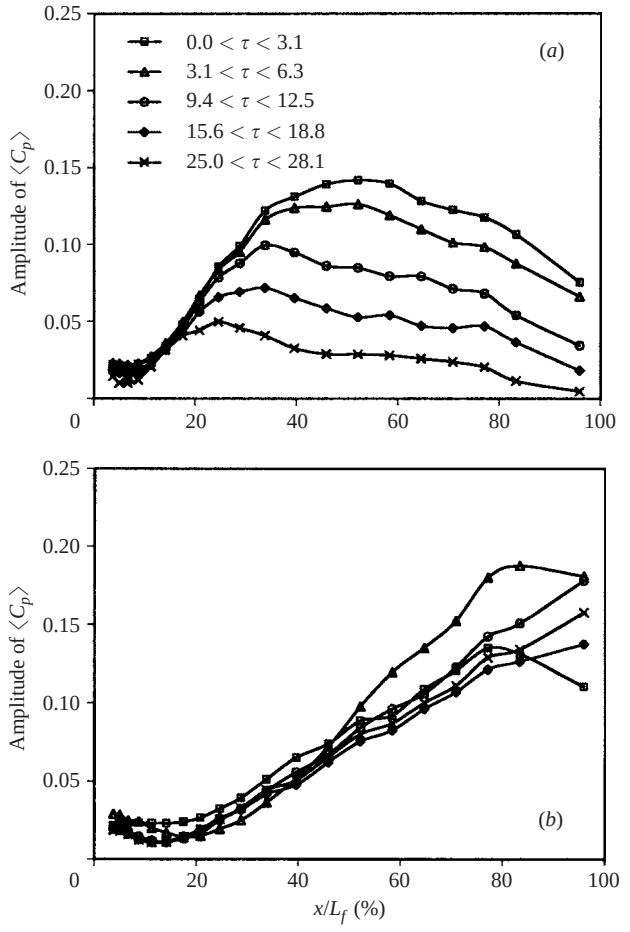

FIGURE 13. Amplitude distribution of wall pressure fluctuations during separation at two forcing conditions; (*a*) $F_r^+ = F_s^+ = 1.2$, $\langle c\mu \rangle_r = 0.02\%$, $\langle c\mu \rangle_s = 0.002\%$; (*b*) $F_r^+ = 1.2$, $F_s^+ = 0.4$, $\langle c\mu \rangle_r = \langle c\mu \rangle_s = 0.02\%$; $\Delta\alpha_s = 5^\circ$.

its original condition in the midst of the process. Switching the excitation to high frequency was used in order to avoid the adverse effect of the dynamic-stall vortex. Three different cases are considered in which the times elapsed from the initiation of the separation to the restoration of the excitation are: $\tau = 5$, $\tau = 12.5$ and $\tau = 25$. The evolution of C_n throughout these processes is plotted in figure 14. In all cases, there is a time lag of $\Delta\tau \approx 3$ from the moment the original excitation was restored until the normal force reverts from its downward slope and starts increasing again. During this time interval, C_n seems to decrease at its normal rate as if no change were made in the excitation (e.g. see figure 1). When the change is made near the mid-point of the separation process ($\tau = 12.5$), the normal force decreases by a relatively large amount ($\Delta C_n = 0.13$) before starting to rise. When the change is made shortly after the initiation of the controlled separation process ($\tau = 5$) or toward its end ($\tau = 25$), the magnitude of the flap off-loading is considerably smaller ($\Delta C_n = 0.03$). If this method is to be used for control purposes, the time delay and its effects can easily be accounted for and corrected within the control scheme.

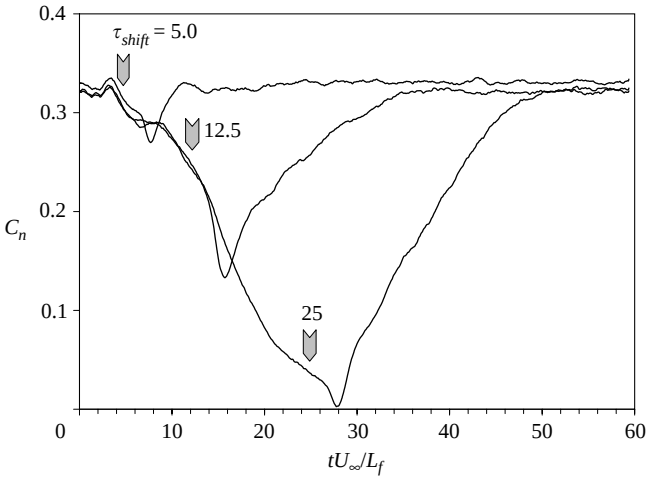

FIGURE 14. Reattachment restored by switching on the disturbance during uncontrolled separation; $Re_L = 1.24 \times 10^5$, $\Delta\alpha_s = 5°$, $F_r^+ = 1.2$, $F_s^+ = 7$, $\langle c\mu \rangle = 0.02\%$.

3. Conclusions

It was demonstrated that abrupt changes in the excitation parameters $\langle c\mu \rangle$ and F^+ that maintain the flow attached over a highly deflected flap could trigger flow separation if the new parameters are incapable in maintaining attached flow. The separation process in these cases may differ appreciably from the separation resulting from a complete cessation of the excitation, since it is still dominated by the excitation. During the initial stage of the unforced separation, a temporary excessive flap load and an associated hinge moment are observed, caused by the development of a large re-circulation zone synonymous with dynamic stall vortex (DSV). Maintaining a certain level of high-frequency excitation corresponding to $3 < F_s^+ < 8$ can completely eliminate the transient excessive loads during the separation process. Low frequencies ($F_s^+ < 1$) work in an opposite direction, increasing the transient load on the flap. At either frequency range, excitation of sufficient amplitude slows down the rate of the separation.

The small-scale eddies enhanced by high-frequency excitation restrain the detachment of the flow near the flap hinge, but they hardly affect the trailing edge area owing to fast spatial decay of their energy. This causes the flow to commence separation at the trailing edge of the flap. By contrast, low frequencies are associated with long wavelengths that are more effective near the aft part of the flap, starting the separation process near the leading edge.

REFERENCES

DARABI, A. & WYGNANSKI, I. 2004 Active management of naturally separated flow over a solid surface. Part 1. The forced reattachment process. *J Fluid Mech.* **510**, 105–129.

GREENBLATT, D., NISHRI, B., DARABI, A. & WYGNANSKI, I. 2001 Dynamic stall control by oscillatory addition of momentum. Part I: Mechanism. *AIAA J. Aircraft* **38**, 439–447.

MCALISTER, K. W., PUCCI, S. L., MCCROSKEY, W. J. & CARR, L. W. 1982 An experimental study of dynamic stall on advanced airfoil sections, Volume 2, Pressure and force data. *NASA TM* 84245.

Nishri, B. & Wygnanski, I. 1998 Effects of periodic excitation on turbulent flow separation from a flap, *AIAA J.* **36**, 547–556.

Nishri, B. 1995 On the dominant mechanism of active control of flow separation. PhD Thesis, Tel-Aviv University.

Sears, W. R. 1956 Some recent developments in airfoil theory. *J. Aeronaut. Sci.* **23**, 490–499.